Proceedings of the IASS 2024 Symposium
Redefining the Art of Structural Design
August 26-30, 2024, Zurich, Switzerland
Philippe Block, Giulia Boller, Catherine DeWolf,
Jacqueline Pauli, Walter Kaufmann (eds.)

Using WAAM Metal Distortion for Sheet Metal Forming

Cedric WEHREN[*a], Johannes KELLERWESSEL[b], Martin TRAUTZ[a],
Rahul SHARMA[b], Uwe REISGEN[b]

[*]Corresponding Author

[a] Chair of Structures and Structural Design (TRAKO), RWTH Aachen University
Schinkelstraße 1, 52062 Aachen, Germany
wehren@trako.arch.rwth-aachen.de

[b] Welding and Joining Institute (ISF), RWTH Aachen University

Abstract

Traditionally, Wire Arc Additive Manufacturing (WAAM) focuses on minimizing distortion [1, 2]. This paper proposes a paradigm shift: leveraging controlled WAAM distortion as a formless method for sheet metal forming, particularly well-suited for fabricating architectural shell structures (Figure 1). WAAM-assisted forming has the potential to improve on-site construction of large building components. Welding robots could precisely adjust pre-cut panels, eliminating bulky formwork and traditional techniques like stretching or hot forming. This approach could also streamline information flow by enabling real-time adjustments for construction deviations. However, accurate simulation data remains crucial for achieving desired geometries

This paper investigates the feasibility of using WAAM for forming shell structures. Toolpath patterns designed to achieve varying degrees of bending were implemented. These patterns were experimentally validated using a welding robot, and a corresponding simulation model was built. Comparison of experimental results with simulations provides deeper insights into material behavior under WAAM influence, enabling the development of more accurate process models. Furthermore, initial strategies for adaptive path planning are discussed to potentially reduce manufacturing errors.

Keywords: DED-Arc, WAAM, material behavior prediction, sheet metal forming, welding

1. Introduction and State of the Art

Achieving resource efficiency in the production of complex, architectural sheet metal structures remains a significant challenge. Even for simple geometrical configurations, formwork costs can be significant, ranging from 25% to 35%, of the total cost of structural work [3]. Although stretch forming offers cost-efficiency due to its durable tooling [4], it becomes impractical for unique, low-volume designs due to high upfront costs associated with custom tooling.

But what if there was a process technology for shuttering-free forming of sheet metal structures? A process that not only eliminates the need for expensive molds but also strengthens the material locally, unlike traditional methods that weaken it through stretching or incremental forming [5]?

Wire Arc Additive Manufacturing (WAAM), a DED-Arc (Direct Energy Deposition) process according to ISO/ASTM 52900, offers a novel approach to sheet metal forming by leveraging residual stress.
However, residual stress, typically considered detrimental in WAAM applications due to potential deformation [6], can be harnessed as a feature for controlled bending. Eliminating the need for costly molds and enabling single-step reinforcement and reshaping of sheet metal. While research has explored re-

inforcing metal sheets using WAAM [7], utilizing deformation itself as a feature is a novel approach within the field. A single-case study from the TU Darmstadt Germany [8] investigated this concept by evaluating the reinforcement of metal sheet facade panels trough WAAM. The study focuesd on the interplay between the degree of reinforcement (number of WAAM layers) and the resulting deformation. In the case study, layer numbers from one to ten were investigated. An increase in deformation was observed up to layer number five, followed by a decrease in deformation up to layer number ten.

In contrast, extensive research has focused on minimizing residual stress in WAAM parts, employing techniques like high pressure rolling [9], post process heat treatment [10], variations in dwell time [11], and optimized tool paths [12]. Conversely, the high accuracy of residual stress prediction [13] unlocks the potential for controlled application in sheet metal forming.

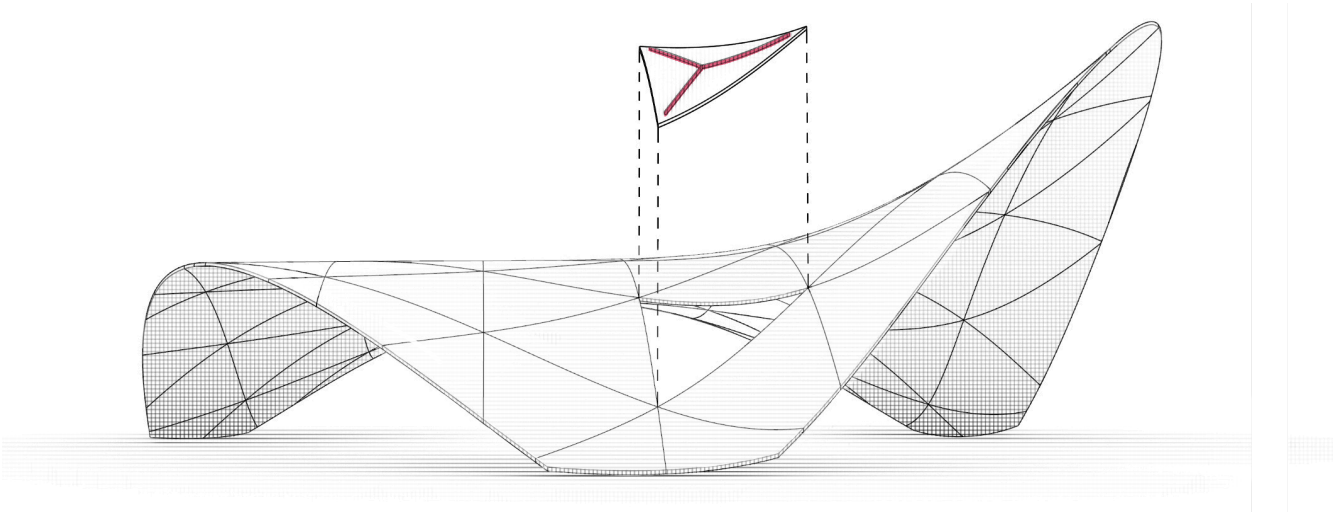

Figure 1: Pavilion with panels bend by WAAM

2. Prediction and Observation of WAAM Bending Behavior

Together with the Welding and Joining Institute (ISF) at the RWTH Aachen University a new process for bending metal sheet using WAAM is being developed. This initial study aims to demonstrate the feasibility of bending sheet metal using Wire Arc Additive Manufacturing (WAAM). To achieve this, different tool path patterns are designed and implemented to create different degrees of one-sided bending from flat sheet metal (details in Section 3.).

These tool path patterns are then used in experimental case studies (Section 4.). Multiple specimens are manufactured using a 6-axis welding robot. The manufactured specimens are 3D scanned and a guiding curve is extracted defined by a curvature κ. This guiding curve is then used in a sequential simulation model (Section 5.).

The simulation model employs data fitting to recreate the observed bending behavior. Simplified bending moments are applied and adjusted both transversely and longitudinally to the weld seam to achieve an accurate simulation. Finally, the simulated data is compared to the extracted experimental data. This comparison provides insights into the bending behavior of sheet metal under the influence of WAAM.

3. Tool path Generation

To achieve the desired curvature (κ) of the sheet metal, unidirectional tool paths are generated. These tool paths rely on several key parameters visualized in Figure 2. The welding seam distance d_i defines the density of the welds, t_i is the weld thickness while α_i describes the orientation of the weld relative to

the principal curvature. For advanced geometries those parameters can vary within a print job. Selection and optimization of these parameters are guided by iterative simulations, as detailed in the next section.

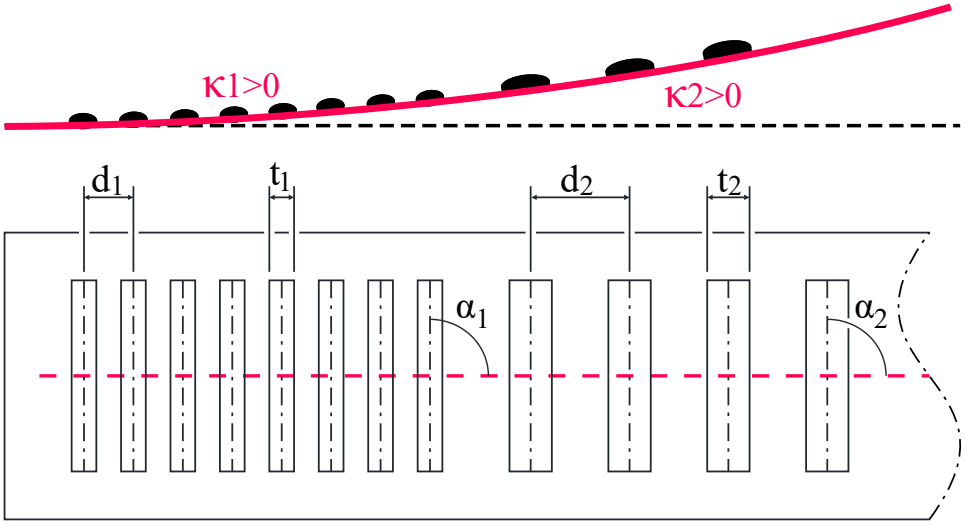

Figure 2: Geometric parameters of unidirectional pattern

4. Experimentation: Observing WAAM Bending Behavior

As part of the research work, three series of tests were carried out, each with three sheets of structural steel S235JR measuring 375x60x2mm. The welds were carried out using a Welbee P502L welding power source and an FD-V8L / NV8L robot from OTC. A synchrofeed process was used for welding. The synchrofeed process corresponds to a controlled short arc process with reversible wire feed. As part of the MSG process, an unalloyed wire electrode of type EN ISO 1434I-A: G42 4 M21/2 C1 3Si1 is welded with a shielding gas consisting of 82% argon and 18% CO_2 of type DIN EN ISO 14175: M21-ArC-18. The welding speed and wire feed are constant across all test series at 0.7 m/min and 3.85 m/min, which corresponds to a welding current of 150 A. The welding data is given in the following table:

Table 1: Welding parameters

Weld power source	Welbee P502L
Roboter	FD-V8L / NV8L
Wire	EN ISO 1434I-A: G42 4 M21/2 C1 3Si1
Gas	DIN EN ISO 14175: M21-ArC-18
Wire feed speed	3,85 m/min
Welding speed	0,7 m/min
specimen material	S235JR
specimen size	375x60x2mm

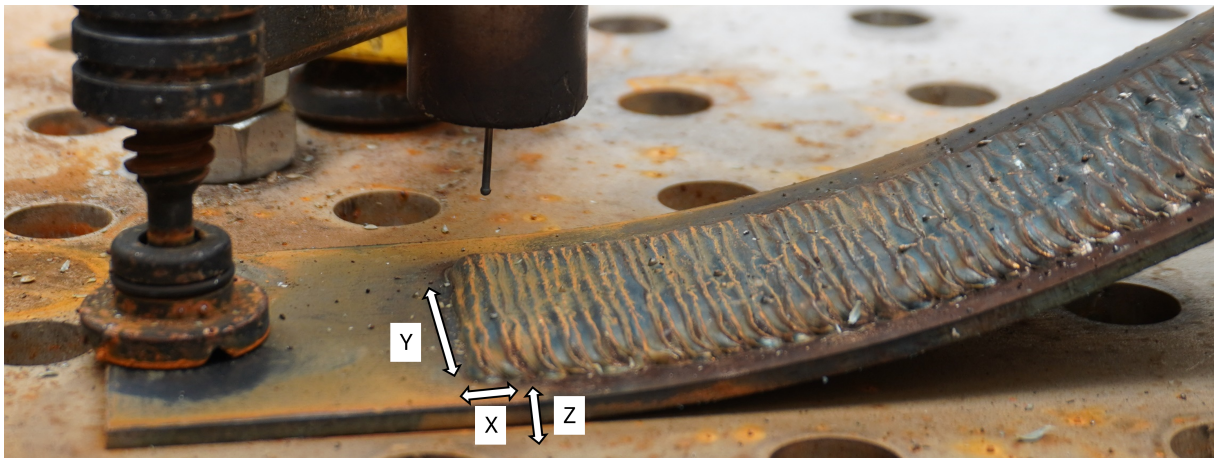

Figure 3: Weld specimen and robot coordinate axis

The torch welds linearly 40 mm along the Y-axis (Figure 3). The component was clamped on one side (Figure 3 left). This meant that the sheet could only bend around the Y-axis. In addition, the one-sided clamping enabled precise positioning of the component and provided a fixed point through which the welding current could flow. The orientation of the welding torch was PA, so the angle between the sheet and the welding wire changed accordingly as the radius of curvature increased. The X and Z distances of the weld seams are varied between the test series. The X distance remains constant within a test series and points in the same directions as distance d_i. The Z-distances of the test series can be approximated by quadratic functions (Figure 4).

After the welding process, the weld seam is cooled to below 100°C by aerosol cooling in order to achieve the fastest possible cooling and reduce the spread of the thermal field [14]. The rapid cooling is intended

to minimise tempering effects in the weld seam and in the base plate in order to achieve the highest possible residual stresses. High stresses enable large deformations.

The Z position of the weld seams in Figure 3 can be described by the quadratic function Equation 1. The table 3 shows the x-distances between the welds. The total length of the welds was 192 mm for all specimens. The number of welds is therefore the total length divided by the distance d_i between the seams.

Table 2: Weld Positions

Value	Case 1	Case 2	Case 3
d_i [mm]	2	4	6
α_i	90°	90°	90°
Welds	96	48	32
M_i	23.187	6.313	1.721

For example, the data for seam $n = 25$ in Case 1 is obtained from the following formula:

$$f(n) = M_i \cdot 10^{-4} \cdot (d_i \cdot n)^2 \tag{1}$$

$$\Rightarrow f(25) = M_1 \cdot 10^{-4} \cdot (d_1 \cdot 25)^2 = 5.797 \tag{2}$$

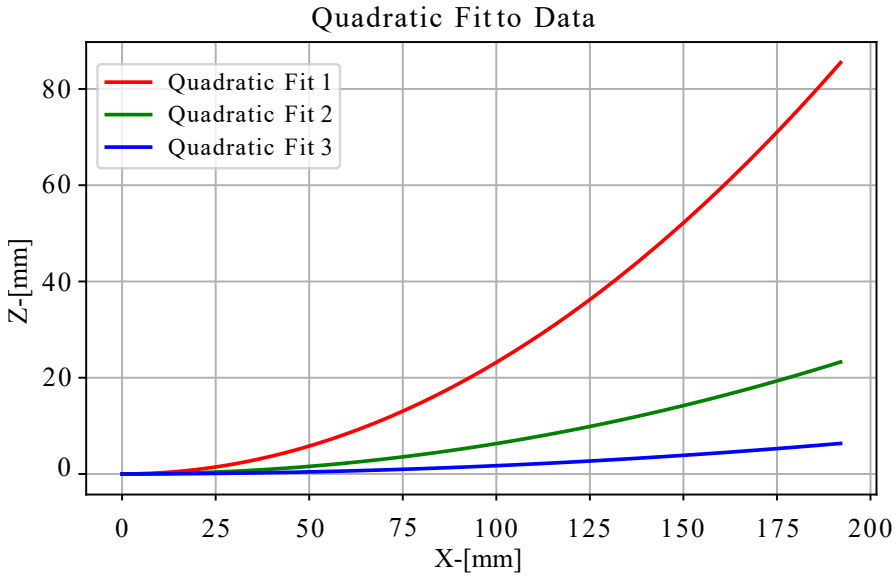

Figure 4: Plot of quadratic function, which determined the Z-Position of the Cases 1-3 from Table 2

Case 1: d_1= 2 mm, κ_1=3.21, α_1=90°

Case 2: d_2= 4 mm, κ_2=1.31, α_2=90°

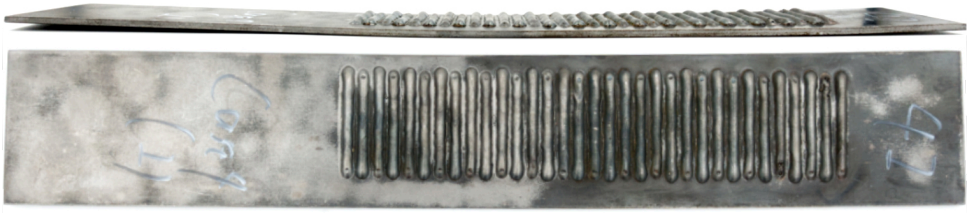

Case 3: d_3= 6 mm, κ_3 = 0.35 , α_3= 90°

Figure 5: Specimens bent using WAAM depositon: Front and top views

5. Simulation: Predicting WAAM Bending Behavior

Wire Arc Additive Manufacturing (WAAM) presents a unique challenge for simulating the bending process. This complexity arises from the intricate interplay of transient thermal stresses and relaxation cycles caused by the heating and cooling cycles during deposition [15, 16]. While predicting final curvature is crucial, WAAM bending simulation goes beyond this. Sheet metal bending relies on gradual deformation, which path planning must consider. Effective simulation can thereby also resolve the sheet´s metal position after each deposition step (material deposition and cooling). This enables generation of an accurate and adaptive tool path, minimizing errors during fabrication.

5.1. Initial Strategy: Single Layer, Single-Curved Geometries

The initial strategy focuses on single-layered, single-curved geometries. The system is discretized into sheet metal and weld sections (denoted as i in Figure 6). Each weld section represents a distinct cool down process simulated in a corresponding simulation step. Details of the controlled cooling process are provided in Section 4.. These subsections are simulated sequentially, considering the deformations and changes in bending stiffness inherited from the previous steps. This sequential approach is later embedded within an iterative optimization loop that refines the overall geometric accuracy of the printed part.

Figure 6: Sheet metal with subsections (i) for sequential simulation, α = 0°

5.1.1. Using Experimental Data for Material Behavior Prediction

To predict material deformation during WAAM bending, the simulation uses data from experimental bending tests conducted under WAAM conditions. This data is used to calculate the bending energy, which is particularly dominant for thin metal sheets like the 3 mm specimens used in the experiments, as nearly all stress converts into bending energy [16]. 3D scans of the specimens' bottom surfaces provide the guiding curvature (κ_i) for the simulation, excluding the clamped section.

5.1.2. Simplified Bending Moments for Efficient Analysis

Accurately capturing the intricate interplay of thermal stresses is one key element for fundamental understanding of how the material behaves during the WAAM process [17]. To address this challenge and enable efficient analysis, this approach utilizes two simplified bending moments, M_{tran} and M_{long}, applied to each weld seam in the simulation (Figure 7). These moments represent thermal induced stresses resulting in bending about axes transverse and longitudinal to the weld seam [16], respectively.

5.1.3. Initial Parameter identification: Isolating bending moments

Data fitting reveals the longitudinal moment, M_{long}, in specimens with a single, continuous longitudinal weld seam parallel to the principal curvature (Figure 8, α = 0°). This minimized the influence of the transverse moment, M_{tran}, allowing us to define the initial moments as: $M_{long} > 0$ and $M_{tran} = 0$.
Next, specimens with orthogonal weld seams (Figure 3, α = 90°) were analyzed to identify M_{tran}. It is important to note that these values are specific to the scenario. Only the bending moment for each weld seam, M_{tran}, was adjustable during calibration, while all geometric parameters were fixed by the specimen characteristics. M_{long} remained constant due to a consistent height and length of the weld seam through the cases.

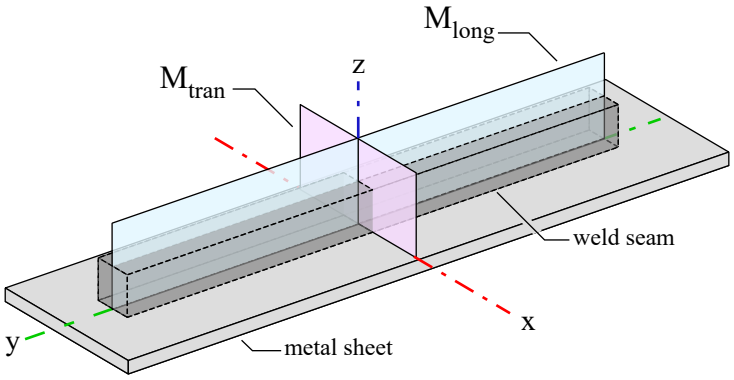

Figure 7: Planes of action of bending moments relative to weld seam

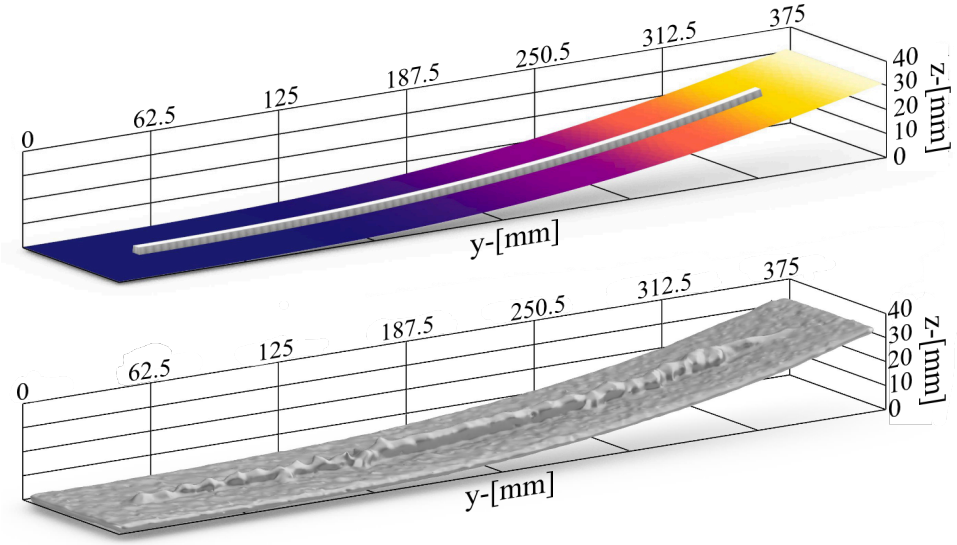

Figure 8: Parallel weld seam ($\alpha = 0°$): Comparison of model simulation (top) with 3D scan (bottom)

6. Results: Comparing Welding Data and Simulation

As seen in Figure 5, different curvatures can be created by only varying between different weld distances as displayed in Table 2. The examined cases involve weld seam distances of 2 mm, 4 mm and 6 mm, while other parameters remained constant. While the increase in weld distance can be described as linear, the extracted curvatures of the specimens shows non-linear behavior: Although Case 2 contains 1.5 times more weld seams than case 3 the curvature rises roughly by factor 4. Case 1 contains 3 times the amount of weld seams compared to Case 3 and has an increased curvature of factor 10.

Figure 9 compares this extracted experimental data with the developed simulation model. While red curves represent the simulated bending curvature, the blue curves represent the guiding curvature averaged out of three identical manufactured specimens per case. The dotted black line represents the extracted boundaries for each case. In case 2 the red simulation curve is almost invisible, laying directly under the blue experimental one. In all three cases, the simulated curve inside its limits defined by the boundaries. It can also be observed, that the variation between individual specimens inside one case becomes more pronounced with increasing curvature.

The calculated bending moments $M_{tran,i}$ for each weld seam show also non-linear behavior, in comparison to the observation from specimens. While the distance between case 1 and case 3 triples, the

calculated bending moments only halves (roughly). It expresses the same phenomenon observed in the experimental studies.

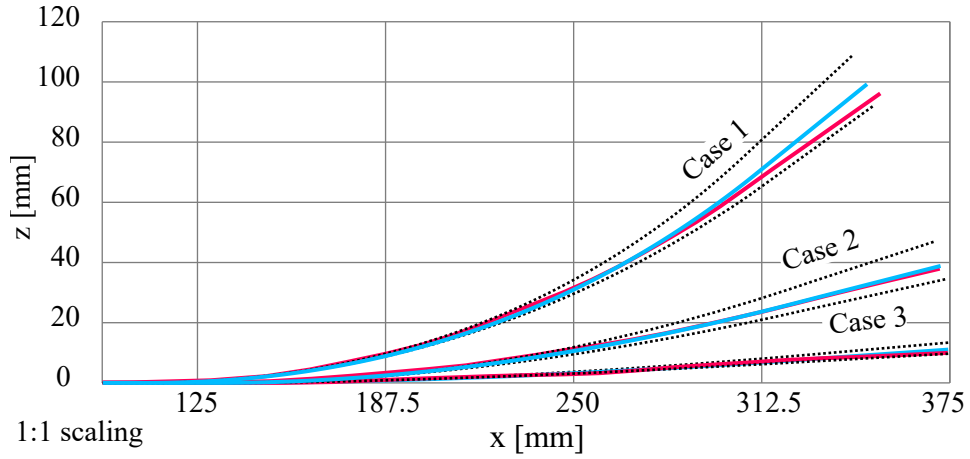

Case 1: $d_1 = 2$mm, $\kappa_1 = 3.21$, $\alpha_1 = 90°$, $M_{tran,1} = 100$ %

Case 2: $d_2 = 4$mm, $\kappa_2 = 1.31$, $\alpha_2 = 90°$, $M_{tran,2} = 78$ %

Case 3: $d_3 = 6$mm, $\kappa_3 = 0.35$, $\alpha_3 = 90°$, $M_{tran,3} = 46$ %

simulation
3d scan (average)
3d scan (boundary)

Figure 9: Orthogonal weld seam: Comparison of model simulation (red) to experimental data (blue)

7. Discussion: Feasibility of Bending Metal Sheets Using WAAM

In this paper the feasibility of bending metal sheets using Wire Arc Additive Manufacturing (WAAM) is demonstrated. Beyond strengthening the metal sheet [7] , WAAM offers the potential to fabricate them into complex, curved shapes.

Non-linear increase in bending forces highlights complexity of this process. To understand and optimise WAAM induced bending more deeply, further parameter studies based on comprehensive data sets are required. These studies can identify key process parameters that influence specific bending scenarios such as layer thickness, number of layers deposited, various welding parameters and the overlap distance of the welds. Simulation coefficients can then be derived from this information. Making it possible to predict how the sheet will react to certain welding sequences.

Future research could also explore integrating 3D scanning or other shape measuring processes into a closed-loop WAAM bending simulation process. After each incremental bending step, the actual shape could be measured and fed back into the simulation, improving accuracy for subsequent steps. Such and adaptive approach can be crucial for WAAM bending, as even identically manufactured specimens exhibit increasing deviations with increasing curvature (Figure 9). By incorporating real-time data, the simulation could continuously refine tool paths, minimizing errors and ensuring successful fabrication of complex geometries [17, 18, 19].

Developing the WAAM bending process for fabricating doubly curved metal sheets is the long-term goal of this research. These sheets hold potential for lightweight shells, such as architecural shell structures (see Figure 1). Another area of application could be the ship building sector or in aviation and aerospace industries.

References

[1] K. Carpenter and A. Tabei, "On residual stress development, prevention, and compensation in metal additive manufacturing," *Materials*, vol. 13, p. 255, 2 2020. DOI: 10.3390/ma13020255.

[2] B. Szost *et al.*, "A comparative study of additive manufacturing techniques: Residual stress and microstructural analysis of clad and waam printed ti–6al–4v components," *Materials Design*, vol. 89, pp. 559–567, 2016. DOI: 10.1016/j.matdes.2015.09.115.

[3] M. Hossain, A. Zhumabekova, S. Paul, and J. Kim, "A review of 3d printing in construction and its impact on the labor market," *Sustainability*, vol. 12, p. 8492, 20 2020. DOI: 10.3390/su12208492.

[4] W. Kuhn, "Untersuchungen über das streckziehen von stahlhülsen mit mehreren ziehringen," 1959. DOI: 10.3929/ethz-a-000090490.

[5] J. Hafenecker *et al.*, "Hybrid process chains combining metal additive manufacturing and forming – a review," *Cirp Journal of Manufacturing Science and Technology*, vol. 46, pp. 98–115, 2023. DOI: 10.1016/j.cirpj.2023.08.002.

[6] M. D. Barath Kumar, "Assessment of process, parameters, residual stress mitigation, post treatments and finite element analysis simulations of wire arc additive manufacturing technique," *Metals and Materials International*, 2022. DOI: 0.1007/s12540-021-01015-5.

[7] P. Grebner and J. Lange, "3d-printing with steel on thin sheets for application in free form façade construction: Welding process development and material properties," *Ce/Papers*, vol. 6, pp. 666–671, 3-4 2023. DOI: 10.1002/cepa.2299.

[8] P. Grebner, L. Riegraf, and J. Lange, "Aussteifung von feinblechen mittels wire arc additive manufacturing für den einsatz im fassadenbau," *DASt-Forschungskolloquium*, vol. 24, pp. 89–92, 2024.

[9] P. Colegrove *et al.*, "Microstructure and residual stress improvement in wire and arc additively manufactured parts through high-pressure rolling," *Journal of Materials Processing Technology*, vol. 213, pp. 1782–1791, 10 2013. DOI: 10.1016/j.jmatprotec.2013.04.012.

[10] S. A. Goviazin G.G. Rittel D., "Achieving high strength with low residual stress in waam ss316l using flow-forming and heat treatment," *Materials Science and Engineering: A*, vol. 873, 2023. DOI: 10.1016/j.msea.2023.145043.

[11] L. R. and X. J., "Influence of interlayer dwell time on stress field of thin-walled components in waam via numerical simulation and experimental test," *Materials Science and Engineering: A*, vol. 25, 8 2019.

[12] K. Mäde, L. Oster, M. Bold, U. Reisgen, and J. Schleifenbaum, "Measurement routine for analysing the thermal impact of additive manufacturing processes on deformation," 2022. DOI: 10.31399/asm.cp.itsc2022p0226.

[13] Q. Wu, "Residual stresses in wire-arc additive manufacturing – hierarchy of influential variables," *Additive Manufacturing*, vol. 35, 2020. DOI: 10.1016/j.addma.2020.101355.

[14] U. Reisgen, R. Sharma, S. Mann, and L. Oster, "Increasing the manufacturing efficiency of waam by advanced cooling strategies," *Additive Manufacturing - Processes, Simulation and Inspection*, vol. 64, pp. 1409–1416, 2020. DOI: 10.1007/s40194-020-00930-2.

[15] T. Rodrigues, V. Duarte, R. Miranda, T. Santos, and J. Oliveira, "Current status and perspectives on wire and arc additive manufacturing (waam)," *Materials*, vol. 12, p. 1121, 7 2019. DOI: 10.3390/ma12071121.

[16] U. Dilthey, "Schweißtechnische fertigungsverfahren 2," 2005. DOI: 10.1007/b139036.

[17] W. Frazier, "Metal additive manufacturing: A review," *Journal of Materials Engineering and Performance*, vol. 23, pp. 1917–1928, 6 2014. DOI: 10.1007/s11665-014-0958-z.

[18] T. Feucht, J. Lange, M. Erven, C. Costanzi, U. Knaack, and B. Waldschmitt, "Additive manufacturing by means of parametric robot programming," *Construction Robotics*, vol. 4, pp. 31–48, 1-2 2020. DOI: 10.1007/s41693-020-00033-w.

[19] N. R. M. Bendia, F. Lizarralde, and F. Coutinho, "Multivariable closed-loop control for layer geometry in wire arc additive manufacturing," *Procedings Do XV Simpósio Brasileiro De Automação Inteligente*, 2021. DOI: 10.20906/sbai.v1i1.2732.

ORC ID:
WEHREN: 0009-0003-3081-6860; KELLERWESSEL: 0009-0008-9433-8876; REISGEN: 0000-0003-4920-2351; SHARMA: 0000-0002-6976-4530; TRAUTZ: 0009-0001-8525-7491